The Development of the "Storm Tracker" and its Applications for Atmospheric High-resolution Upper-air Observations

Wei-Chun Hwang[1] Po-Hsiung Lin[1] and Hungjui Yu[1]

[1] Department of Atmospheric Sciences, National Taiwan University, No. 1, Sec. 4, Roosevelt Road, Taipei, Taiwan, 106.

Correspondence to Po-Hsiung Lin (polin@ntu.edu.tw)

https://scholars.lib.ntu.edu.tw/cris/rp/rp07764

Abstract

In this study, we introduce a newly-developed upper-air observational instrument for atmospheric research. The “Storm Tracker” (or “NTU mini-Radiosonde”), is an ultra-lightweight (about 20g including battery), multi-channel simultaneous capable radiosonde designed by the Department of Atmospheric Sciences at National Taiwan University. Developed since 2016, the Storm Tracker aims to provide an alternative for observation of atmospheric vertical profiles with a high temporal resolution, especially lower-level atmosphere under severe weather such as extreme thunderstorms and tropical cyclones.

Field experiments were conducted as trial runs at Wu-Chi, Taichung, Taiwan, to examine the ability of the Storm Tracker on boundary layer observation, in addition to the intercomparison between the Storm Tracker and the widely used Vaisala RS41-SGP radiosonde. Among the co-launches of the Storm Tracker and Vaisala RS41 radiosondes, the measurements of pressure, wind speed, and wind direction are highly consistent between the Storm Tracker and Vaisala RS41-SGP. However, a significant daytime warm bias was found due to solar heating. A metal shield specifically for the Storm Tracker was thus installed and showed mitigation for the warm biases and the overall variance.

With the much lower costs of the radiosondes and the simultaneous multi-channel receiver, the Storm Tracker system has shown great potential for high-frequency observational needs in atmospheric research.

1. Introduction

With a long history of development, the upper-air radiosonde has been one of the essential and the most reliable method to measure the atmosphere above us so far. Operational weather agencies worldwide share their daily to twice-a-day (00UTC and 12UTC) radiosonde observational data through WMO GTS (Global Telecommunication System) for synoptic weather analysis and numerical model forecast. According to the European Centre for Medium-Range Weather Forecasts (ECMWF), in 2017, there are about 818 upper-air radiosonde stations worldwide in addition to more than twelve radiosonde manufactures (Ingleby 2017). So far, most radiosonde manufacturers had participated in the field inter-comparison program hosted by World Meteorological Organization (WMO) throughout 1984–2010, and there were 11 different types of operational radiosondes processed in the recent inter-comparison experiment at Yangjiang, China in 2011 (Nash et al. 2011)

Among all different types of radiosondes, the mostly used Vaisala RS41 radiosonde weighs 110g, and the previous version RS92 weighs 280g. The Japan radiosonde from Meisei Corporation, iMS-100 weighs 38g only, which is so far the lightest operational radiosonde. However, occasionally there are needs for many radiosondes within a short period of time to acquire higher temporal resolution data. For the atmospheric research community, most of these radiosondes on the market are often a burden regarding the research budget when a large amount is needed. Secondly, the lighter the radiosonde weighs, the smaller the balloons and the less the helium is needed. Lighter radiosondes also enable launching using a low-cost constant plastic balloon, which can also be deployed as a drift-sonde. In section 4, we will present two scenarios, one is vertical profiling, and the other is drift-sonde operation.

In this study, we introduce a newly-developed, smaller, lighter, and cheaper upper-air radiosonde system designed with the capability of simultaneously receiving multiple radiosondes, which is explicitly for high temporal resolution observations on mesoscale

weather systems. This so-called Storm Tracker system, developed at the Department of Atmospheric Sciences at National Taiwan University, has been tested in several field experiments since 2016. In section 2, the configuration of the Storm Tracker system is described in detail. Trial runs of preliminary comparisons between the Storm Tracker and the Vaisala RS41-SGP radiosonde are discussed in section 3. Section 4 concludes the current status of the Storm Tracker system and its applications in different field campaigns. Section 5 is the concluding remarks.

2. Configuration for Storm Tracker Upper-air Observation System

The Storm Tracker upper-air observation system is described in this section, which consists of the upper-air radiosonde (the Storm Tracker) and the surface signal receiving unit (the Ground Receiver). Figure 4 shows the system block diagram of the Storm Tracker system.

a. The Storm Tracker radiosonde

The Storm Tracker radiosonde is packed with sensors and supporting hardware, as shown in Figure 5. The main portion includes the ATMEGA328p microcontroller, the U-blox MAX7-Q GPS sensor, the Bosch BMP280 pressure sensor, the TE-Connectivity HTU21D temperature-humidity sensor, and the LoRa™ transmitter.

The main processor of the Storm Tracker is the Microchip ATMEGA328p microcontroller (Atmel Corporation 2015). The microcontroller processes all measurements from the sensors and sends them to the radio transmitter.

For the GPS module, the U-blox MAX-7Q is selected (U-Blox 2014). This GPS module provides the altitude and speed as well as the direction of the Storm Tracker. The overall GPS module possesses an accuracy of 2.0 m for horizontal position and 0.1 m/s for velocity (U-Blox 2014).

The pressure sensor on the Storm Tracker is Bosch BMP280, with an overall operation range from 1100 to 300 hPa and from –40 to 85℃, in addition to a typical accuracy of ±1hPa (Bosch Sensortec 2018). This sensor has been applied widely to indoor navigation, where a precise pressure measurement is required.

For the sensor of temperature (T) and relative humidity (RH), we used the HTU21D, a digital relative humidity sensor with temperature output from TE Connectivity. This sensor is chosen regarding its high accuracy (±0.3℃ in T and ±2% in RH), wide operational range (–40 to 125℃, 0–100%), the short response time (5 seconds), and cutting-edge energy-saving property (TE Connectivity 2017). The HTU21D sensor is located at the 3-cm arm, as shown in Figure 5, to extend outside of the protection box to measure the environment. Table 3 briefly summarizes the operational ranges and typical accuracies of atmospheric measurements for the Storm Tracker and the Vaisala RS41-SGP radiosonde (VAISALA Corporation 2017).

The power for Storm Tracker comes from one AAA battery, and this minimizes the total weight. The radio transmitter is powered by LoRa™, which is a long-range, low-power wide-area network technology (Augustin et al. 2016). The radio frequency used by Storm Tracker ranges from 432MHz to 436.5MHz, the configuration for LoRa™ is 7 for spreading factor (SF) and 4/5 for code rate (CR) with 125kHz channel bandwidth. SF and CR, along with the channel bandwidth, define the transmission speed. Specifically, SF indicates the system's ability to receive the signal with a low Signal-to-Noise Ratio; the larger the number, the higher the sensitivity. For the Storm Tracker system, we set the SF to the lowest number of 7 in order to speed up the baud rate and make it enough for the communication range ~100km. Lastly, to extend the battery life to several hours, the transmit power is set to 18 dB with 1 Hz of transmission frequency.

As for the Storm Tracker enclosure, we use thick white paper with anti-water coating. Facing the temperature and humidity solar radiation biases found during the trial runs in 2017,

we design a 1-mm thick tinplate metal shield to cover the temperature and humidity sensors to prevent direct solar radiation. The detail of the metal shield added to the Storm Tracker sonde is shown in Figure 6. The complete package of the Storm Tracker and the enclosure with the metal shield is shown in Figure 4.

For the production, a local printed circuit board (PCB) assembly factory manages the production of both the Storm Tracker and the Ground Receiver. The final cost of each Storm Tracker sonde (~50 USD) is about one-tenth of the price of a regular Vaisala RS41-SGP radiosonde as purchased in Taiwan.

Furthermore, since the Storm Tracker only weighs about 20g, including a battery, it can be easily carried by a constant volume foil balloon for constant-height flight, or pilot rubber balloon for regular upper-air observation. Figure 5 shows a typical Storm Tracker launch with a pilot rubber balloon, and Table 4 summarizes the Storm Tracker properties.

b. The Ground Receiver

We also designed a ground receiver to receive and process the data from Storm Tracker, the right panel of Figure 1 shows the system block diagram of the ground receiver. The RF module, as shown by the green block, will capture the incoming RF (Radio Frequency) signal, and we use the same RF module for Storm Tracker as the receiver. The package will then be sent to MCU for data parsing before being sent to the MPU (Main Processing Unit). The MCU we choose is the same as Storm Tracker (ATMEGA328p), and the MPU is a WiFi capable MT7688 SoC (System on Chip). MPU hosts the Web server and records the data to the external micro SD card. The power source can be either a USB power supply or a wide range of DC power supply (3~16 Volt) through DC Jack. Figure 6 shows a complete set of Storm Tracker Ground Receiver installed in a 3D-printed box (9cm*2cm*5cm). The Ground Receiver is then connected to an omnidirectional antenna with 6dB gain. A typical setup of the Ground Receiver in the field is shown in Figure 7.

The most powerful feature of the Storm Tracker system is the ability to receive data from up to ten radiosondes simultaneously, which provides the opportunity of upper-air observations with extremely high temporal/spatial resolution. In a word, one can launch up to ten Storm Trackers at once with only a receive; or launch a series of Storm Trackers in a short period, say an hour, 30 minutes, or even 10 minutes depending on the mission.

To accomplish this goal with a single-channel transceiver on the Storm Tracker, time-divided multi-access (TDMA) was implemented into the Storm Tracker system. Since each Storm Tracker takes about 76ms for data transmission, the system splits every second into 10-time slots, and each Storm Tracker transmits the data on the different time slots pre-assigned during Storm Tracker manufacture programming. Therefore, the Ground Receiver is constantly scanning ten different frequencies per second and tracking up to ten Storm Trackers at the same time.

A newer version of the Ground Receiver is currently underway, which is powered by Raspberry Pi and a unique in-house designed LoRa™ gateway, which can receive 8-channel simultaneously. In the future, this new design with TDMA could monitor 80 Storm Trackers at the same time.

c. The launch procedure

Nevertheless, the Storm Tracker system is still under development and testing. Here we present the launch and ground check procedure for the latest intercomparison field experiment. First, we install the battery and place the Storm Tracker at a location that it can receive the GPS signal. Once the GPS signal has been received, the data will be transmitted and show up on the receiver's webpage. The user can check if the measurements are correct as in other radiosonde launching processes, such as the Storm, Tracker ID number, battery voltage, and the instrument data. The Storm Tracker is then clear to launch.

The overall setup of the Storm Tracker system before the actual launch is relatively easy and takes less amount of time (~10 min) comparing to a regular Vaisala ground system. This also shortens the preparation time for the observation of short-term weather events such as thunderstorms.

3. The intercomparison between the Storm Tracker and Vaisala RS41-SGP

a. Field experiment design

Two trial field experiments were conducted to examine the performance of the Storm Tracker system on the boundary layer (BL) observations. In these trial runs, we attached the Storm Tracker to the side of RS41-SGP by double-sided foam tape, with the sensor arm of Storm Tracker sticking out from the main body, as shown in Figure 8. The first trial run was conducted for four days in December 2017 at Wu-Chi, Taichung, Taiwan, and in total 28 sets of Storm Tracker and Vaisala RS41 were launched. One of the results from this trial run is the solar radiation affecting the temperature and moisture measurements. Therefore, we installed a thin metal shell (i.e., the "hat") around the temperature/humidity sensor, as shown in Figure 6, to prevent the direct solar heating in the second trial run conducted at the same location in July 2018. During the second run, every launch includes a Vaisala RS41 attached with two Storm Trackers, one with and one without the hat. Similar to the first run, the data from 19 co-launches under the clear sky were collected, the average vertical profile from the Vaisala RS41 shows a clear signature of subsidence and an overall dry atmosphere (Figure 9). In this section, the data from the second run will be shown to examine the performance by adding the metal shield.

b. Humidity time-lag error analysis

Since both the Storm Tracker and the Vaisala RS41-SGP transmit data every second, we could first analyze the time lag error for humidity. The analysis is done by separating the time-series data into three different altitude sections: 200m to 3000m, 3000m to 4500m and >

4500m. For each section of the time-series, we find the resulting delay that maximizes the cross-correlation. To exclude the effect of solar radiation heating, we use only the nighttime data to calculate the time-lag. The average time-lags are shown in Table 4.

One example of the time-series is shown in Figure 11. We could see that for humidity without the metal shield, the time lag is about 5 to 8 seconds. And the higher the altitude, the longer the time-lag. Furthermore, in the case of adding the metal shield, the time-lag is longer compared to the case without a metal shield, which indicates that the metal shield might affect the ventilation, but overall the time-lag is still small around 7 to 9 seconds.

c. Temperature and humidity solar radiation biases analysis

The raw data from both Storm Tracker and Vaisala RS41-SGP were analyzed by calculating the difference along with the time series. For calculating the mean and standard deviation of the biases across different altitudes, the Vaisala RS41 altitude data was used as the reference, and the vertical profiles are from 200m to 6000m at a 20m interval. The data during daytime (8–18 LST) and nighttime (18–8 LST) were separated to see how the sensor response to solar radiation. The vertical profiles of Temperature and Humidity biases are shown in Figure 10, and the statistics are in Table 3.

First, we can see from Figure 10(a) that either with or without the metal shield, the temperature, and humidity sensor had experienced significant solar heating during the daytime, which also caused the solar radiation dry bias (Vömel et al. 2007) in moisture measurements. Furthermore, temperature bias increases with altitude. Overall, with the metal shield added, the standard deviation and mean of the biases are smaller at most altitudes (Figure 10(c)). As shown in Table 3, during the daytime, the mean temperature warm bias drops from 2.98℃ to 2.61℃ by adding the hat. The standard deviation also drops from 1.61℃ to 1.23℃. Likewise, the mean dry bias drops from 3.47% drier to 2.43% drier with the hat. Moreover, the standard deviation

decreases from 6.44% to 5.3%. These results show that the reflective metal shield does help to prevent direct solar heating when the Storm Tracker is in the air.

However, the installation of the metal shield causes a further warm bias when there is no solar heating. From Figure 10(b), we can see that the case with the metal shield experienced a warm bias in the profile, which also caused the humidity moist bias to drop and brought down the overall humidity difference. In Table 3, the mean warm bias increases from 0.16℃ without the hat to 1.29℃ with the hat, and the standard deviation increases from 0.39℃ to 0.54℃. The mean humidity bias, on the other hand, drops from 5.63% moister for Storm Tracker without the hat to 1.82% for Storm Tracker with the hat. In both cases, the standard deviation is similar ~3.5%. During the nighttime, the results show that the metal shield further induces a warm bias, which may be the leading cause of the drying moist bias.

Finally, we look at Figure 10(c), and we can see the benefit of lowering the variances of measurements by adding the metal shield onto the temperature/humidity sensor. In Table 3, on average, even though mean warm bias increases from 1.52℃ to 1.93℃ if the hat is added, the standard deviation decreases from 1.82℃ to 1.15℃. Moreover, the mean humidity bias improves from 1.23% to -0.23% with the hat, and the standard deviation also drops from 6.84% to 4.92% with the hat.

Even though the metal shield causes a slight warm bias during the nighttime, it mitigates the solar radiation heating effects and the solar radiation dry bias during the daytime when most of the mesoscale convective rainfall occurs. For such events in Taiwan, it is worthwhile to apply these new instruments to acquire much higher resolution data, especially for afternoon thunderstorms triggered by daytime solar heating.

d. Pressure and GPS analysis

Since the Vaisala RS41-SGP is equipped with a pressure sensor, we also compared our BMP280 sensor with that of the Vaisala RS41-SGP, as shown in Table 5. Although the

resulting initial error is higher than BMP280's accuracy, we tried to mitigate the difference by applying a ground check procedure on the pressure measurements for each launch. As indicated in Table 5, the resulted pressure measurements were further improved that the mean pressure error drops from 2.76 hPa to 0.33 hPa for Storm Tracker without the hat, and the trend is the same for Storm Tracker with the hat. In addition, for the measurements derived for the GPS, the Storm Tracker performs very well comparing to the Vaisala RS41-SGP, as shown in Table 5.

4. Applications in the field campaigns

One of the main scientific purposes of the experiments conducted is to examine the performance of the Storm Tracker system on the BL observations. In Figure 12, we present the time-height series data across the experiment timeline. The colors represent θ_e, and the arrow represents the wind speed and direction. The BL heights (gray lines) were calculated according to the method described in Liu and Liang (2010). Here we can see that the evolution of the boundary layer grows and maximized near noon. Moreover, with the higher temporal resolution of ~3-hourly, we could see the diurnal cycle of the development of the boundary layer. This demonstrates one of the use cases for Storm Tracker in gathering high temporal or spatial data enabled by the ability of simultaneous signal receiving.

Another campaign during typhoon Talim on September 13, 2017, was conducted with three Storm Trackers to see if the observations inside the tropical cyclones are possible. As shown in Figure 13, light-weighted Storm Tracker can be launched with a conventional and small constant balloon, which then can stay afloat at a fixed atmospheric layer. Figure 13 shows the flight path and the altitude of the Storm Tracker into the typhoon. In this experiment, the Storm Tracker stayed at 6200m for about 1 hour. Although the signal was lost eventually by the mountains blocking between the receiver and the Storm Tracker, this launch shows the potential of Storm Tracker to conduct drift sound experiments in the future.

5. Concluding remarks

Although the Storm Tracker system is incorporated with the new low-cost sensors, we show that it can accomplish decent performance compared with Vaisala RS41 radiosonde with a significant cost reduction. Moreover, with the capability of tracking multi-tracker simultaneously and incorporating LoRa™ technology, it enables future missions to deploy many radiosondes to collect higher temporal/spatial resolution data.

These trial runs show that the Storm Tracker radiosondes still have issues regarding temperature and moisture measurements. Still, the current configuration with a thin metal shield does help with the daytime biases and lowering the variance. More experiments to compare the measurements between the Storm Tracker and Vaisala RS41 are underway, in addition to the intercomparison among different individual instruments such as radiometer. More importantly, with more intercomparison data, the objective correction algorithms are currently developed and tested for better data quality control.

Data availability

All field measurement data from our Storm Tracker and Vaisala RS-41-SGP could be accessed through FTP by request.

Authors contribution

Mr. Hwang makes the PCB, program coding, and document draft. Dr. Lin supports all funding of this study and coordinated field tests. Dr. Yu joins the discussion of data intercomparison.

Competing interests

The authors declare that they have no conflict of interest.

Acknowledgments

The authors would like to thank the RS-41 data sharing from RCEC (Research Center for Environmental Changes) in Academia Sinica, and the field test supported by TASSE program

(MOST 108-2119-M-002-022) which is managed by Prof. Hung-Chi Kuo, National Taiwan University. We also appreciate the efforts of the associate editor and the anonymous reviews whose comments to improve this paper

References

Atmel Corporation, 2015: ATmega328P 8-bit AVR Microcontroller with 32K Bytes In-System Programmable Flash Datasheet. ATmega328P [DATASHEET] 7810D–AVR–01/15, 294 pp, http://ww1.microchip.com/downloads/en/DeviceDoc/Atmel-7810-Automotive-Microcontrollers-ATmega328P_Datasheet.pdf.

Augustin, A.; Yi, J.; Clausen, T.; Townsley, W.M., 2016: A Study of LoRa: Long Range & Low Power Networks for the Internet of Things. Sensors, 16, 1466. https://doi.org/10.3390/s16091466.

Bosch Sensortec, 2018: Datasheet BMP280 Digital Pressure Sensor. BST-BMP280-DX001-19, 49 pp, https://ae-bst.resource.bosch.com/media/_tech/media/datasheets/BST-BMP280-DS001.pdf.

Ingleby, B.,2017: An assessment of different radiosonde types 2015/2016. ECMWF Technical Memoranda, 807. Pp77.

MediaTek, 2016: MediaTek MT7688 Datasheet, 294 pp, http://labs.mediatek.com/en/chipset/MT7688

Nash, J., Oakley, T., Vömel, H., & Wei, L., 2011: WMO intercomparison of high quality radiosonde systems, Yangjiang, China, 12 July–3 August 2010. World Meteorological Organization, Instruments and Observing methods, report No, 107.

TE Connectivity, 2017: HTU21D(F) RH/T SENSOR IC Digital Relative Humidity sensor with Temperature output. HTU21D(F) RH/T SENSOR IC, 22pp, https://www.te.com/commerce/DocumentDelivery/DDEController?Action=showdoc&DocId=Data+Sheet%7FHPC199_6%7FA6%7Fpdf%7FEnglish%7FENG_DS_HPC199_6_A6.pdf%7FCAT-HSC0004.

U-Blox, 2014: MAX-7 u-blox 7 GNSS modules Data Sheet. UBX-13004068, 24 pp, https://www.u-blox.com/sites/default/files/products/documents/MAX-7_DataSheet_%28UBX-13004068%29.pdf.

VAISALA Corporation, 2017: Vaisala Radiosonde RS41-SGP. B211444EN-E, 2pp, https://www.vaisala.com/sites/default/files/documents/WEA-MET-RS41SGP-Datasheet-B211444EN.pdf.

Vömel, H., H. Selkirk, L. Miloshevich, J. Valverde-Canossa, J. Valdes, E. Kyrö, R. Kivi, W. Stolz, G. Peng, and J. A. Diaz (2007), Radiation dry bias of the Vaisala RS92 humidity sensor, J. Atmos. Oceanic Technol., 24, 953âAŠ963.

Shuyan , Liu, and Liang Xin-Zhong. “Observed Diurnal Cycle Climatology of Planetary Boundary Layer Height.” Journal of Climate, vol. 23, 2010, pp. 5790–5809., doi:10.1175/2010JCLI3552.1.

Caption List

Table 1. List of the operational ranges and typical accuracies of basic atmospheric measurements for Vaisala RS41-SGP radiosonde (VAISALA Corporation 2017) and the Storm Tracker.

Table 2. Characteristics of Storm Tracker.

Table 3. Temperature and Humidity Error (Storm Tracker minus Vaisala RS41-SGP) Statistics for the second intercomparison experiment in July 2018 at Wu-Chi.

Table 4. Average time-lag for the second intercomparison experiment in July 2018 at Wu-Chi.

Table 5. All the sensor error (Storm Tracker minus Vaisala RS41-SGP) statistics for the second intercomparison experiment in July 2018 at Wu-Chi.

Figure 1. System block diagram for the Storm Tracker system, including Storm Tracker (left) and Receiver (right). The part number for the chipset is indicated in the box, and the arrow indicated the dataflow.

Figure 2. Photo of a PCB assembled Storm Tracker product from the PCBA. The diameter of the Storm Tracker is 58.1mm x 50.2mm (height x width, including sensor arm). The GPS antenna and GPS module are located on the top right of Storm Tracker, along with the power switching on the top left. The RF module is located on the bottom, and the red wire is the quarter-wave antenna. The extended arm hosts the temperature and humidity sensor, and the

pins on the bottom are for programming and debug purposes. Lastly, in the middle are the microcontroller and pressure sensor.

Figure 3. A closeup picture of the metal shield. The metal shield is a 15mm x 15mm x 15mm square cube, and the inner sensor PCB is a 7mm x 7mm square.

Figure 4. A Storm Tracker with the enclosure and the metal shield. The enclosure is composed of paper, and the hole on the top (bottom) is for connecting to the balloon (passing of the antenna). The metal shield is attached to the PCB board with hot glue.

Figure 5. A Storm Tracker (without enclosure) launched with a pilot rubber balloon (20g) during a field campaign.

Figure 6. Photo of a Storm Tracker Ground Receiver. On the right are the GPS module and RF module to receive the signal, along with the USB and DC power jack for power input and the console access. In the middle is the central processor, which handles data recording and hosts the website. On the left is the SD card for storage. On the top are the indicator LEDs, which show the current status of the receiver and the received data channels.

Figure 7. A typical setup of the ground receiver in the field, with the 433Mhz antenna in the middle, and the receiver, GPS antenna and power bank at the bottom black box.

Figure 8. A photo of the intercomparison launch setup. The Storm Tracker is attached to the side of a Vaisala RS41 radiosonde with double side tape.

379 Figure 9. The skew-T-log-P diagram of the average vertical profile measured by Vaisala RS41
380 radiosondes during the intercomparison run in July 2018 at Wu-Chi. The thick red line
381 indicated the dew point, and the thick blue line indicated the temperature profile.
382
383 Figure 10. (a) top (b) middle (c) bottom The vertical profiles for temperature and humidity
384 differences during both the daytime and nighttime in July 2018 at Wu-Chi experiment. The
385 lines indicated the mean, and the one standard deviation ranges are shaded. The red color
386 indicates daytime data, and blue color indicates nighttime data.
387
388 Figure 11. One of the launch data for time-lag analysis, the original time-series data, is at the
389 top. And the time-lag corrected time-series in the middle, with three segments of the time series
390 data for three altitude bins. And lastly, the altitude to time-lag plot at the bottom.
391
392 Figure 12. The time-series-height data for the experiment done during July 2018 at Wu-Chi.
393 The shaded color represents $\boldsymbol{\theta_e}$ and the arrow direction indicates wind direction with length
394 indicate the wind speed. Lastly, the gray line is the boundary height calculated with the
395 algorithm developed by Liu and Liand in 2010.
396
397 Figure 13. Three balloon tracks during Typhoon Talim (top) and the height profile of the Storm
398 Tracker 0 (bottom). The height profile at the bottom is the time series data with time at the x-
399 axis and height(meter) at the y-axis. The launching site is located on the campus of National
400 Taiwan University. The maximum range of the Storm Tracker from the site is 132km, in which
401 the Storm Tracker could maintain at about 6200m height. Credit to Google Earth Pro for
402 providing the satellite image.

403 **Tables**

404

405 **Table 3. List of the operational ranges and typical accuracies of basic atmospheric**
406 **measurements for Vaisala RS41-SGP radiosonde (VAISALA Corporation 2017) and the**
407 **Storm Tracker.**

408

Spec	Vaisala RS41-SGP	Storm Tracker
P Range	sfc. - 3 hPa	1100 - 300 hPa
P Accu.	1.0 hPa (>100 hPa)	1 hPa (0 - 65 ℃)
		1.7 hPa (-20 - 0 ℃)
T Range	-90 - +60 ℃	-40 - +125 ℃
T Accu.	0.3 ℃ (<16 km)	0.3 ℃
	0.4 ℃ (>16 km)	
RH Range	0 - 100 %	0 - 100 %
RH Accu.	4%	2%
Horizontal WIND SPEED Accu.	0.15 m/s	0.1 m/s
		(Hor. Accu.: 2.5 m)

409

410

411 **Table 4. Characteristics of Storm Tracker.**

412

Characteristic	Storm Tracker
Sensors	Temperature, Humidity, Pressure, GPS location, Wind Speed
Frequency	432 MHz to 436.5 MHz
Channels	Ten simultaneous Channels
Time Resolution	1s (1Hz)
Power	1x AAA Battery
Battery Life	2 - 4 Hours
Weight	20g with 1x AAA Battery
Dimension	58.1 mm x 50.2mm x 30mm

413

414

Table 3. Temperature and Humidity Error (Storm Tracker minus Vaisala RS41-SGP) Statistics for the second intercomparison experiment in July 2018 at Wu-Chi.

	Temperature Error (˚C)		Humidity Error (%)	
	W/o hat	With Hat	W/o hat	With Hat
Night Time	0.16±0.39	1.29±0.54	5.63±3.46	1.82±3.45
Day Time	2.98±1.61	2.61±1.23	-3.47±6.44	-2.43±5.3
Total	1.52±1.82	1.93±1.15	1.23±6.84	-0.23±4.92

418 **Table 4. Average time-lag for the second intercomparison experiment in July 2018 at Wu-**

419 **Chi.**

Configuration	Height				
	200~3000m	3000~4500m	4500m~end	Average	
With Hat	6.90	7.50	8.80	7.73	Seconds
Without Hat	4.70	5.60	7.80	6.03	Seconds

420

421 **Table 5. All the sensor error (Storm Tracker minus Vaisala RS41-SGP) statistics for the**

422 **second intercomparison experiment in July 2018 at Wu-Chi.**

	W/o hat	With Hat
Temperature (°C)	1.52±1.82	1.93±1.15
Humidity(%)	1.23±6.84	-0.23±4.92
Pressure(hPa) *initial	2.76±1.29	2.59±1.5
Pressure(hPa) *with offset	0.33±1.06	0.43±1.71
Speed(m/s)	0.037±0.628	0.046±0.521
Direction(degree)	1.19±26.5	0.595±28
Height(m)	-4.5±16.7	-3.4±19.3

423

Figures

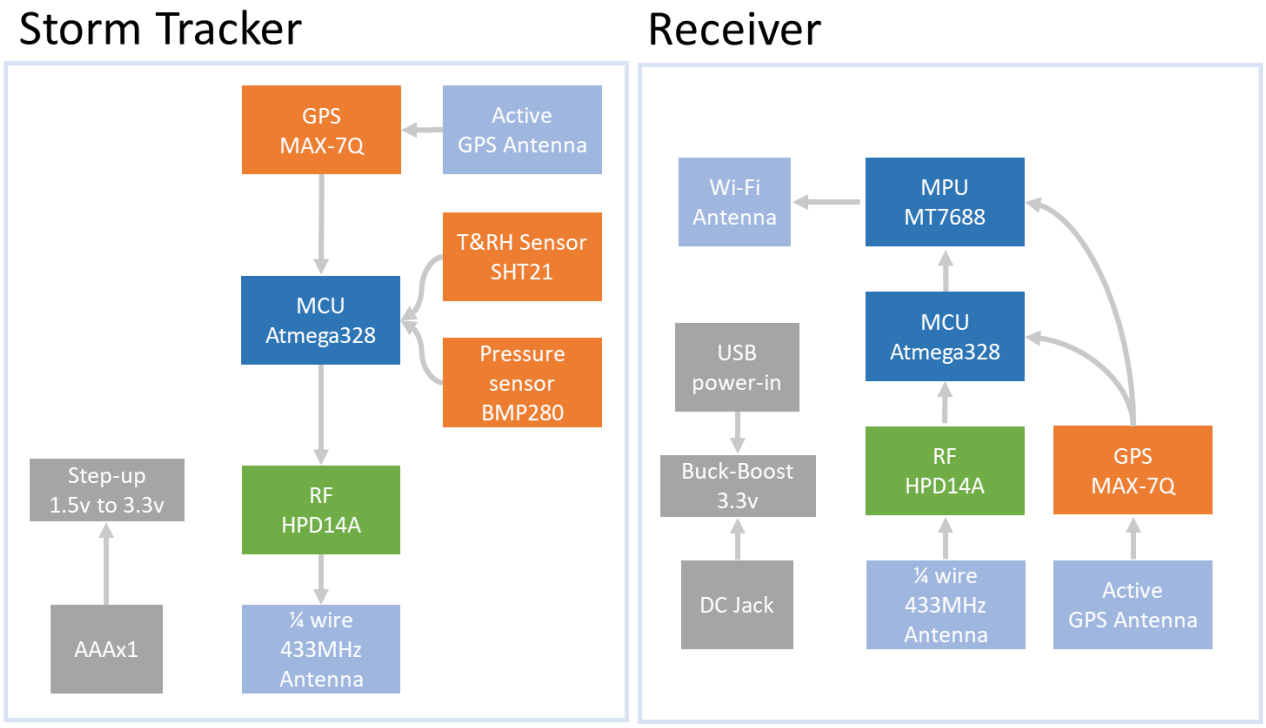

Figure 4. System block diagram for the Storm Tracker system, including Storm Tracker (left) and Receiver (right). The part number for the chipset is indicated in the box, and the arrow indicated the dataflow.

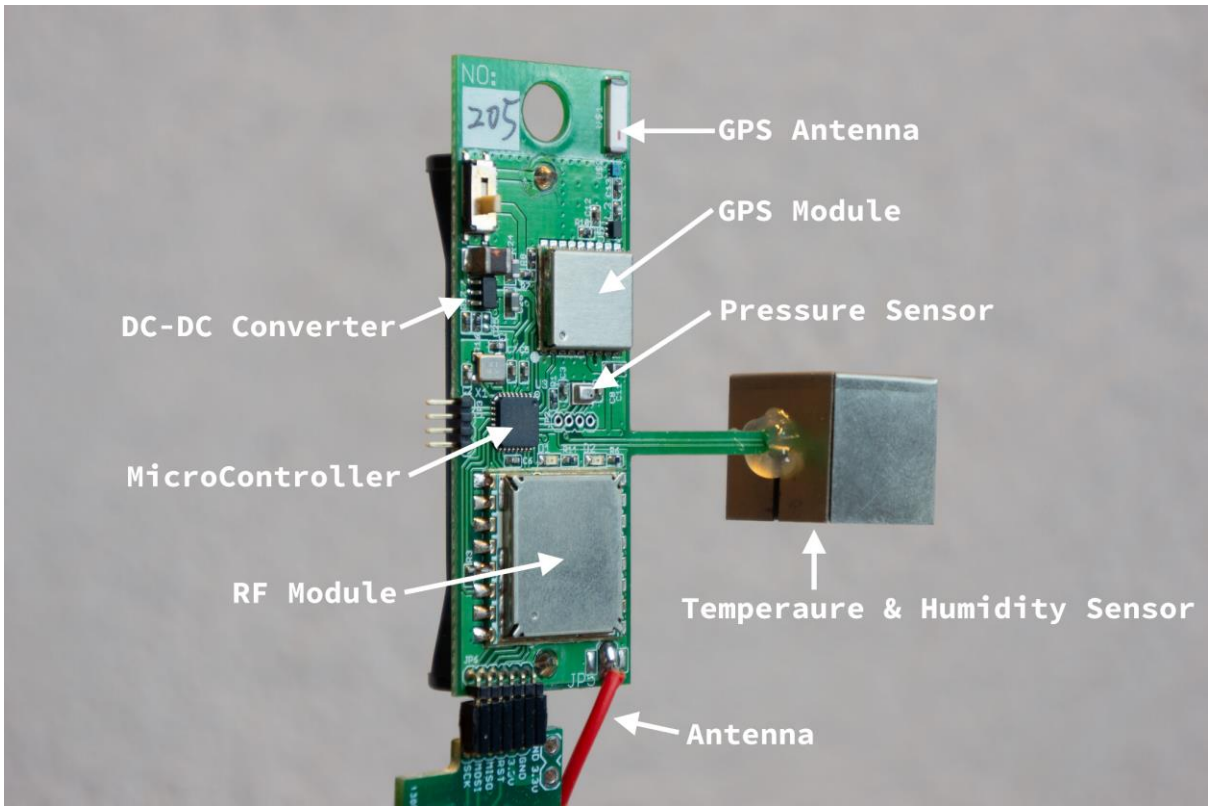

Figure 5. Photo of a PCB assembled Storm Tracker product from the PCBA. The diameter of the Storm Tracker is 58.1mm x 50.2mm (height x width, including sensor arm). The GPS antenna and GPS module are located on the top right of Storm Tracker, along with the power switching on the top left. The RF module is located on the bottom, and the red wire is the quarter-wave antenna. The extended arm hosts the temperature and humidity sensor, and the pins on the bottom are for programming and debug purposes. Lastly, in the middle are the microcontroller and pressure sensor.

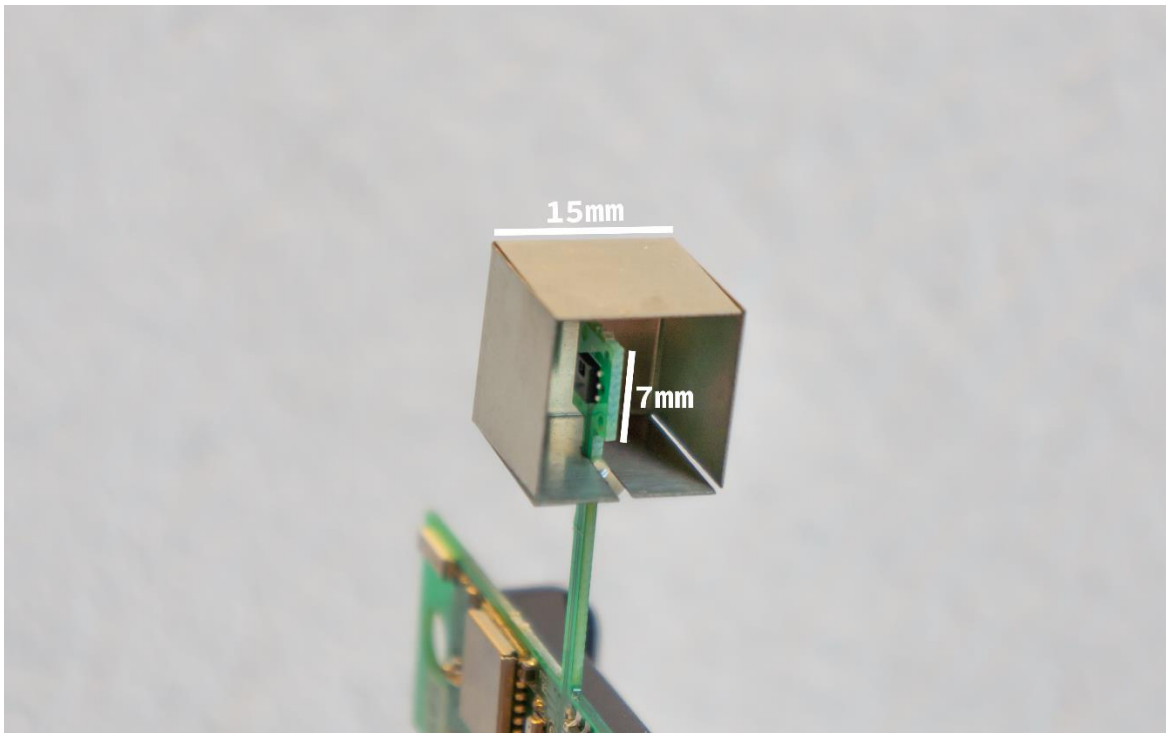

Figure 6. A closeup picture of the metal shield. The metal shield is a 15mm x 15mm x 15mm square cube, and the inner sensor PCB is a 7mm x 7mm square.

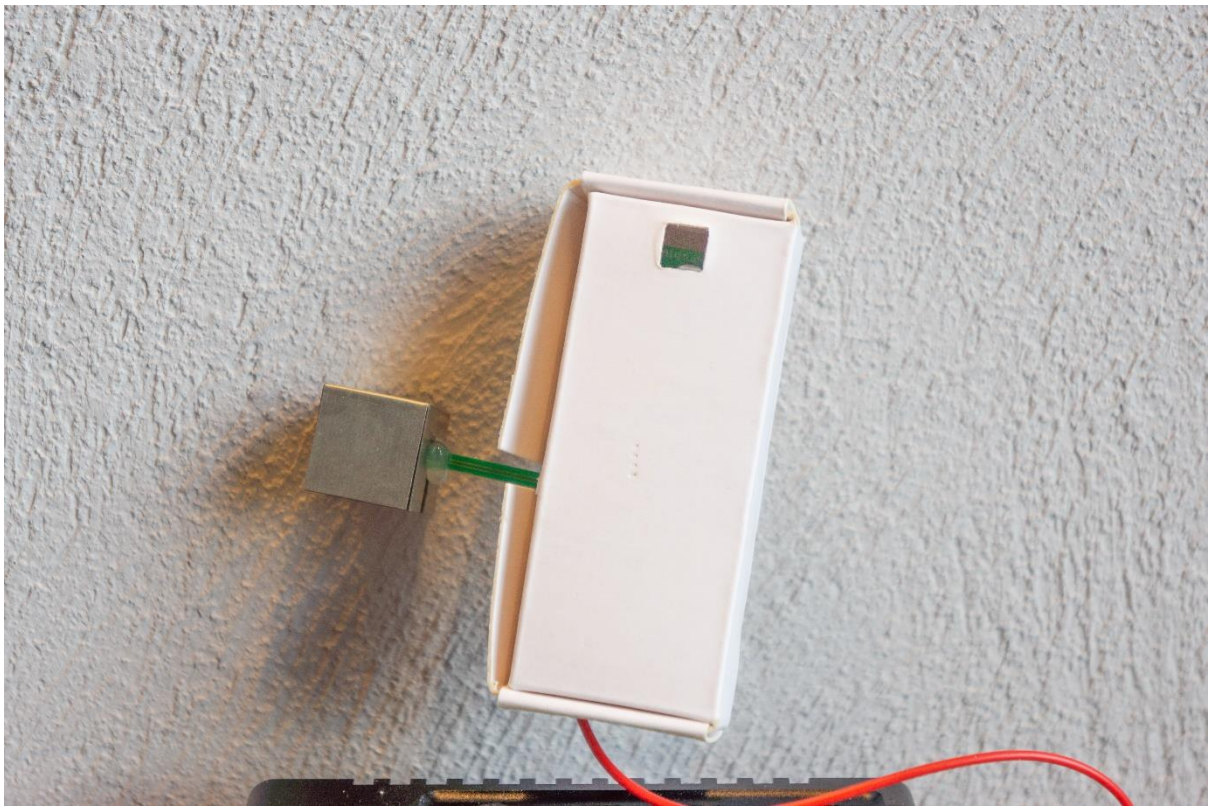

Figure 4. A Storm Tracker with the enclosure and the metal shield. The enclosure is composed of paper, and the hole on the top (bottom) is for connecting to the balloon (passing of the antenna). The metal shield is attached to the PCB board with hot glue.

Figure 5. A Storm Tracker (without enclosure) launched with a pilot rubber balloon (20g) during a field campaign.

Figure 6. Photo of a Storm Tracker Ground Receiver. On the right are the GPS module and RF module to receive the signal, along with the USB and DC power jack for power input and the console access. In the middle is the central processor, which handles data recording and hosts the website. On the left is the SD card for storage. On the top are the indicator LEDs, which show the current status of the receiver and the received data channels.

466

467

468 **Figure 7. A typical setup of the ground receiver in the field, with the 433Mhz antenna in**

469 **the middle, and the receiver, GPS antenna and power bank at the bottom black box.**

470

Figure 8. A photo of the intercomparison launch setup. The Storm Tracker is attached to the side of a Vaisala RS41 radiosonde with double side tape.

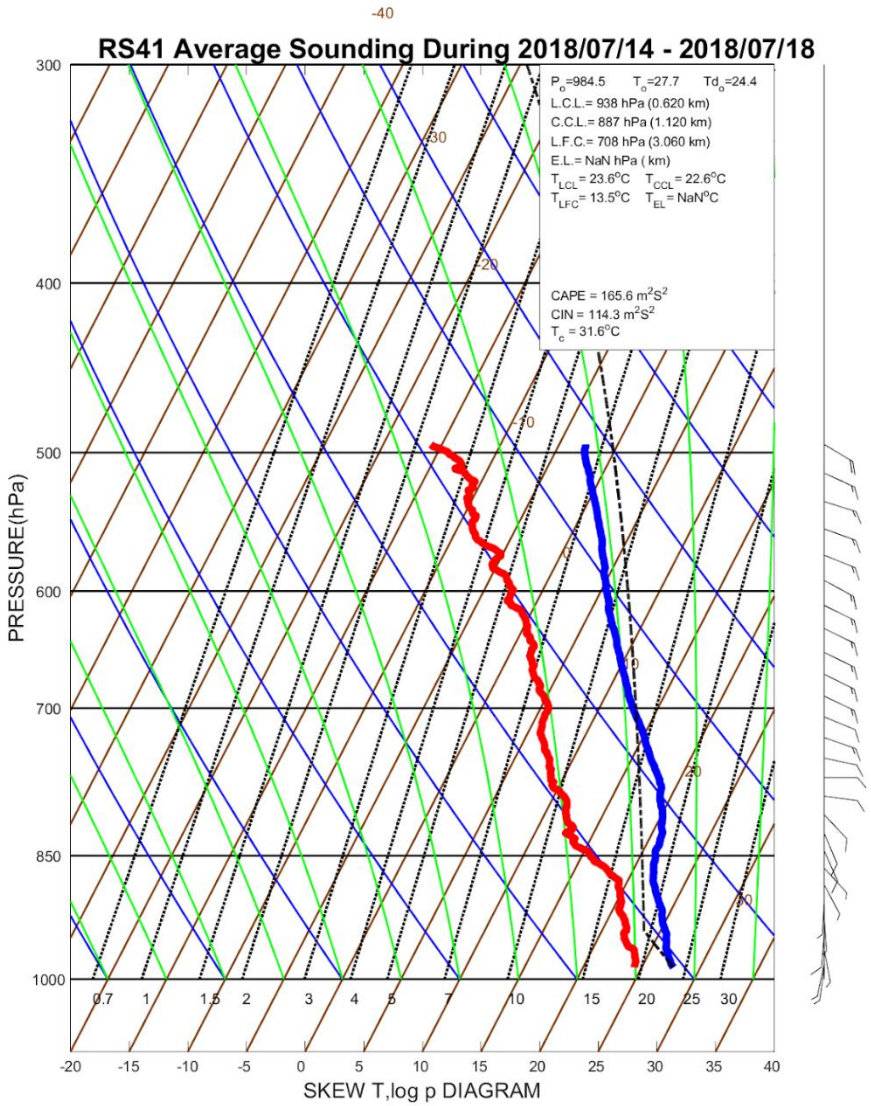

Figure 9. The skew-T-log-P diagram of the average vertical profile measured by Vaisala RS41 radiosondes during the intercomparison run in July 2018 at Wu-Chi. The thick red line indicated the dew point, and the thick blue line indicated the temperature profile.

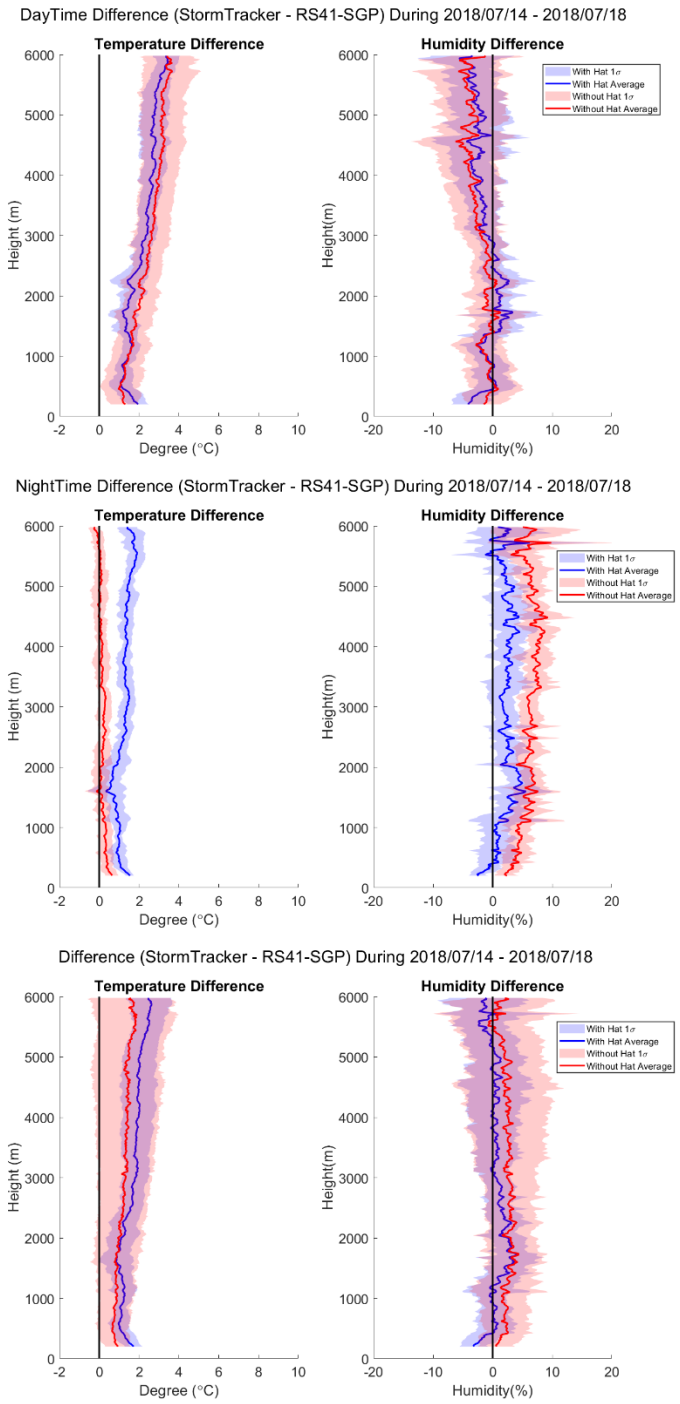

Figure 10. (a) top (b) middle (c) bottom The vertical profiles for temperature and humidity differences during both the daytime and nighttime in July 2018 at Wu-Chi experiment. The lines indicated the mean, and the one standard deviation ranges are shaded. The red color indicates daytime data, and blue color indicates nighttime data.

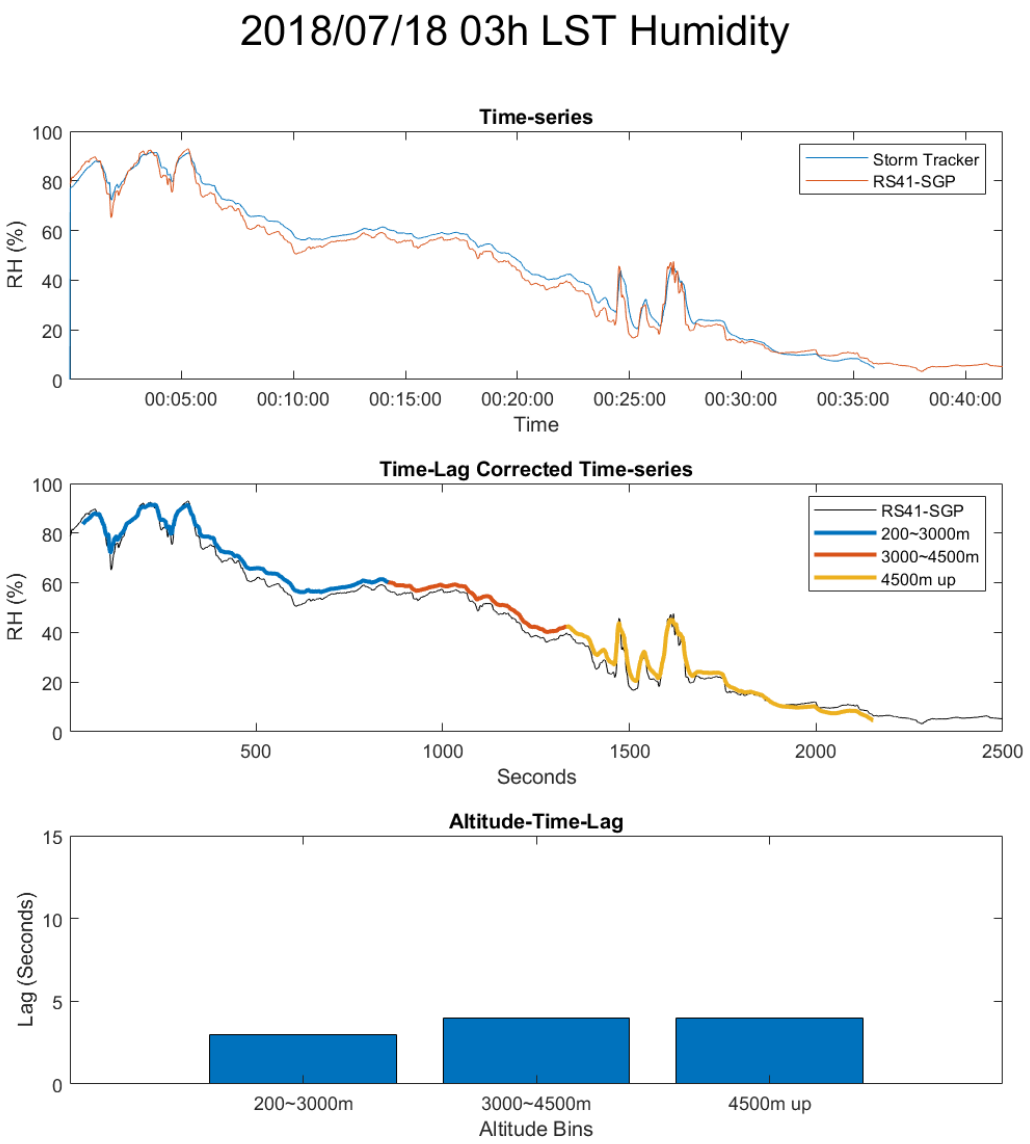

Figure 11. One of the launch data for time-lag analysis, the original time-series data, is at the top. And the time-lag corrected time-series in the middle, with three segments of the time series data for three altitude bins. And lastly, the altitude to time-lag plot at the bottom.

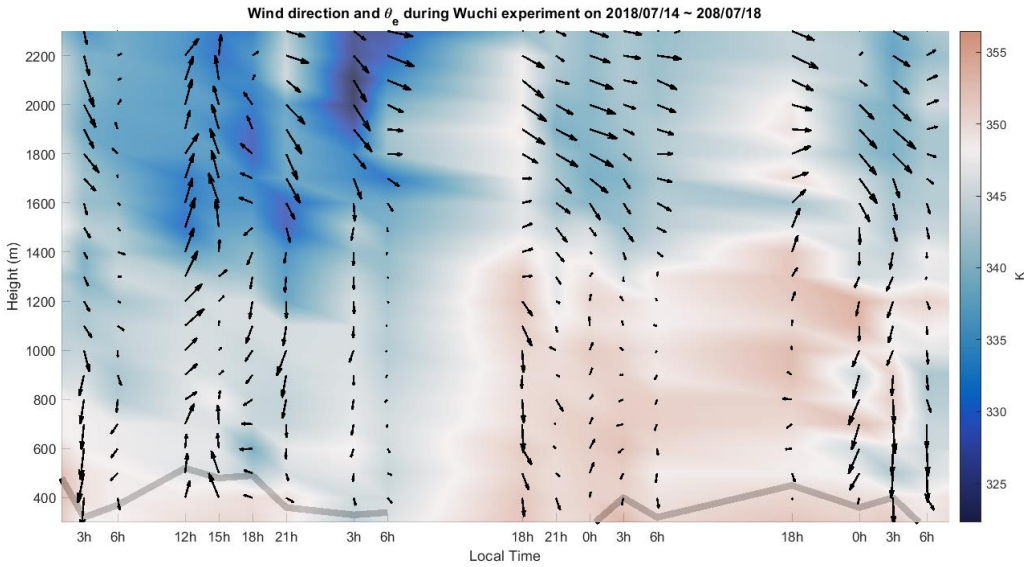

493

494 **Figure 12. The time-series-height data for the experiment done during July 2018 at Wu-**
495 **Chi. The shaded color represents θ_e and the arrow direction indicates wind direction**
496 **with length indicate the wind speed. Lastly, the gray line is the boundary height calculated**
497 **with the algorithm developed by Liu and Liang in 2010.**

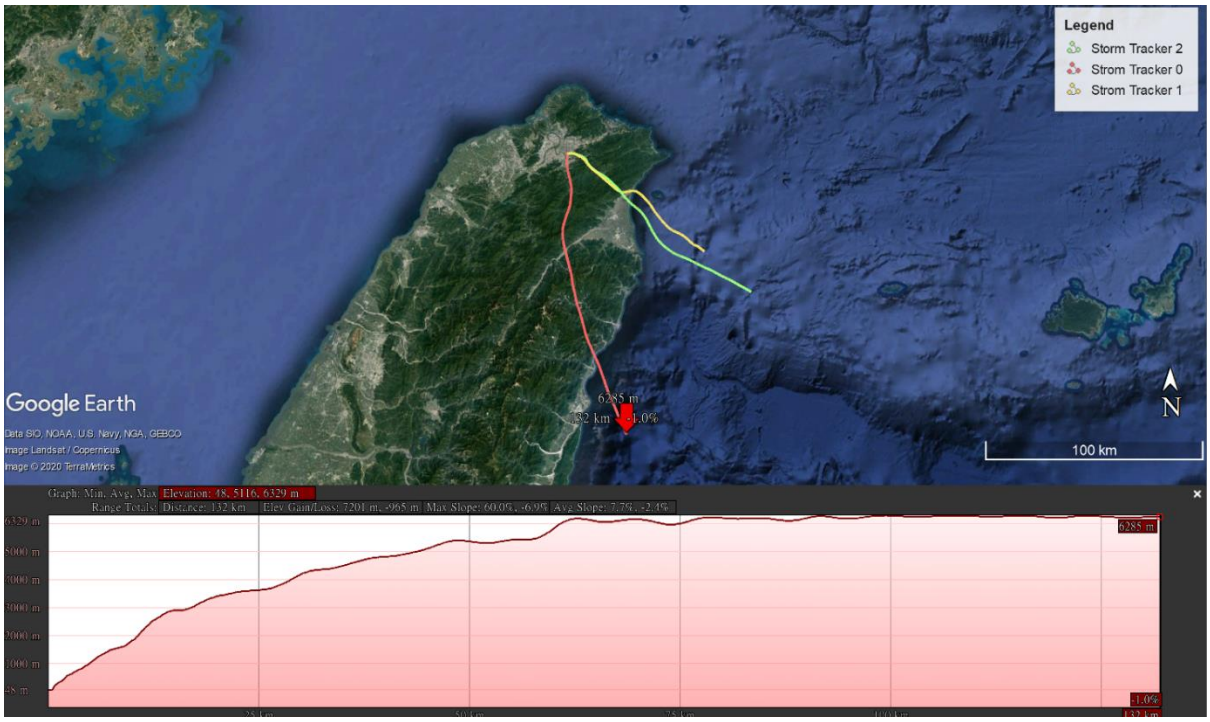

Figure 13. Three balloon tracks during Typhoon Talim (top) and the height profile of the Storm Tracker 0 (bottom). The height profile at the bottom is the time series data with time at the x-axis and height(meter) at the y-axis. The launching site is located on the campus of National Taiwan University. The maximum range of the Storm Tracker from the site is 132km, in which the Storm Tracker could maintain at about 6200m height. Credit to Google Earth Pro for providing the satellite image.

This paper describes at an in-depth technical level the development of a low-cost radiosonde built using standard off the shelve parts. The low-cost values of such a system is one novel point. The second is the potential to have several in the air at a time allowing a swarm approach to measurements in the troposphere. However the scientific reward of this is poorly demonstrated.

Thank you very much for your time and efforts reviewing this study, we modified our paper according to your following comments.

The technical description is quite thorough and in depth and should be simplified through the use of tables and using more general descriptions of the components used so that an audience from a wide community can understand the description

Thank you for the comment. We slightly simplified section 2, although we think the details are important and serve as a reference for future research.

In Section 3 this can be better presented in terms of figures used. It appears the authors have got all the data they need to undertake a comprehensive comparison and they've missed the mark a bit. Firstly, I'd like to see a plot of vertical profiles of temperature and RH (Use RH and avoid Dewpoint as Dewpoint is derived from the RH on the RS41) from both the Storm tracker and RS41 on the same plot for day / night cases and with and without the protective screen. Avoid using a skew-T diagram as these are a function of pressure. Instead use the GPS height from both the storm tracker and RS41. They have similar Ublox systems within once you take the covers off.

Thank you for the suggestions, we rewrote and reorganized section 3 as follows according to the comments from you and another reviewer, Dr. Masatomo Fujiwara.

First, the discussions for the trial experiment in December 2017 are removed in the updated manuscript. It is because we found the results consistent with those in the second trial which consists of additional comparison w/wo the hat. In the updated manuscript, we focus on the analyses for the second trial experiment in July 2018.

Next, we now have all the Vaisala RS41-SGP and the Storm Tracker data at the same time coordinate. After calculating the means and standard deviations within the same height range, we show the vertical profiles of T and RH differences (Day, Night-

time, and total) in the updated Figure 10. And the averaged measurements are shown in the following figures (Fig1,2,3).

We still keep the skew-T diagram in the updated Figure 9 as a reference for the average weather condition during the experiment.

Also, the standard RS41 does not contain a pressure sensor. It back infers pressure from GPS using the hydrostatic balance. Unless it is an RS41 GP which does contain a pressure sensor, probably worth checking when undertaking a comparison with the BMP280.

Thank you. We used the Vaisala RS41-SGP, as indicated in the paper. In the updated manuscript, we compared the RS41-SGP pressure sensor with the BMP280 in Table 5 along with the discussion in Section 3d.

The histograms are good. However, the real story appears in the profile plots (Fig 10-13). I'd suggest moving the histograms to a supplementary figure and using the profile plot differences instead.

We modified the section 3 accordingly.

Section 4 is somewhat confusing, when I began reading it I was expecting to see a case study where a swarm of sensors had been launched and a temperature contour map at a given pressure surface would be displayed for a given altitude or pressure. Or a height time temperature contour map. However, only the trajectories were plotted. I feel to highlight the novelty of this work a preliminary result showing either temperature, humidity or wind component as a function of height or area is needed.

Following on from this Section 4 seemed to also be the conclusions. Section 4 and the conclusions need to be in two separate sections.

Section 4 is now modified as suggested. In addition to the intercomparison between the Storm Tracker and the Vaisala RS41-SGP, the experiments in Wu-Chi was aimed to explore the variation of the PBL. We added a paragraph in section 4 discussing this.

Nevertheless, the results are so far preliminary, more case studies using the Storm Tracker are currently underway, especially during the Taipei Summer Storm Experiment (TASSE) in 2018–2019. In a word, we focus on the overall performance of the Storm Tracker in this manuscript.

There are numerous typos and grammatical errors that also need rectifying some are highlighted below:

Line 30 and throughout: Strom should be Storm

Corrected.

Line 49-55: I suggest making a table here with the various radiosondes and their weights and potential cost per sonde.

Thank you for the comment, although we want to present the table with various radiosondes, most manufacturers would not publicly share their unit cost. Moreover, bulk buying will impact the cost per radiosondes a lot, so we couldn't present such a table.

Lines 52-55: You need to be clearer here about what kind of field campaigns you are on about. What are you trying to measure that would make a normal radiosonde not fit for the job both logistically and financially? (I think you make a case for it further down in this section. But I'd bring that argument earlier on)

Thank you for the comment, we clarified in the discussion.

Line 82: MCU , I guess you mean Micro Control Unit. You need to define this.

Updated.

Line 92: Remove the from before TE

Updated.

Line 102-104: I'm not familiar with the LORA technology but saying thins like setting is 7 for spreading factor and 4/5 for code rate, will not yield any useful information to

the general reader. Either describe in everyday terms what these settings mean or relegate to supplementary material. Do however included the baud rate

Thank you for the comments, the spreading factor(SF) along with code rate(CR) defines the baud rate of LoRa. Unlike Narrow Frequency Modulation or other similar modulation which may only need to indicate the bandwidth and baud rate, LoRa modulation is able to do a tradeoff between the baud rate and the required SNR to receive the signal, which is indicated using SF. Simply write down the baud rate of the resulting configuration will miss a lot of details about the system's immunity to the noise. We added the discussion about the un-common settings for LoRa in section 2 according to your comments.

Line 117-129: Figure 1b shows a nice block diagram. I advise to rewrite this paragraph stepping through and describing how the received signal is parsed through the system. At each stage describe in simple terms what each part of the circuit does. For example, say the main CPU is a MT7688 (The configuration is not that important)

Thank you for the comment, we updated the discussion herein.

Line 151: attached

Updated.

Reference:

https://www.vaisala.com/sites/default/files/documents/WEA-MET-RS41SGP-Datasheet-B211444EN.pdf

This paper introduces a newly developed, low-cost radiosonde instrument called Storm Tracker. This is a very interesting development and has a potential to be a useful tool for atmospheric science in the future. I have a few major comments and some minor comments on the current manuscript, some of which may be suggestions for future work.

Thank you very much for your time and efforts in reviewing this study, Prof. Masatomo Fujiwara. We've updated our paper according to your following comments.

Major comments:

(1) Please show some typical, individual profiles, together with the simultaneous RS41 profiles for all the variables. Here, time, rather than height, is appropriate as the independent variable. Such figures would show the actual response time, as well as possible biases, of the measurements of each variable by the Storm Tracker. For example, were the temperature inversion and the relative humidity drop at the top of the planetary boundary layer quantitatively captured? (It should be noted that relative humidity, rather than dew point temperature, should be evaluated because for both radiosondes, relative humidity should be the primary measurement.)

Thank you for the suggestions, for the response time issue, we added the section 3b to discuss the response time for humidity measurements.

Here we show all of the other variables for the StormTracker with hat co-launch on 2018/07/15 18h local time. The orange line is the RS41-SGP, and the blue line is Storm Tracker. The time lag indicates in the figure shows that the time-lag for humidity is not significant.

his study introduces a new radiosonde “Storm Tracker” for vertical profiles measurements in the atmosphere. The study fits the scope of Atmospheric Measurement Techniques. The new sensor shows similar accuracy and resolution compared to Vaisala RS41, while being lighter and more economical. The manuscript is well written. I have only a few minor comments. Minor comments Line 19 “upper-air observational instrument”; Lines 24-25 “especially lower-level atmosphere”. Which one is more accurate? Upper-air or lower-level? Lines 186-197. Adding the metal shield decreases the temperature bias from 2.47 ◦C to 2.18 ◦C in the daytime, but increases the temperature bias from 0.13 ◦C to 1.17 ◦C. I am not sure if adding the metal shield is worthwhile since the daytime bias decrease is much smaller than the nighttime bias increase in terms of percentage. In particular, adding the metal shield increases the temperature bias to 9 times of that without it at night. Figure 13 The texts in legends are too small.

Thank you for the time reviewing this study and the comments

For the terms “upper-air” and “lower-level”, the term “upper-air” used among the radiosonde community indicates that the sensing device (like Strom Tracker) goes up with a balloon or a kite, in contrast to “dropsonde” which goes down from an aircraft. So both descriptions about Strom Tracker are not contrasting to each other, but “upper-air” means it is a radiosonde observing while going upward, and the term “lower-level” means it targets to low-level atmosphere observations.

For adding the metal shield, even though it increases the mean bias during nighttime, the overall variance is lower. Nevertheless, the Storm Tracker sonde is still under early development stage and the design is flexible at this point. In addition, a comprehensive correction procedure is currently underway.

Finally, Fig. 10 (previous Fig.13) is updated according to your comments.